Neuro-Oncology
21(6), 800–808, 2019 | doi:10.1093/neuonc/noz037 | Advance Access date 6 February 2019

Septal dysembryoplastic neuroepithelial tumor: a comprehensive clinical, imaging, histopathologic, and molecular analysis

Jason C. H. Chiang, Julie H. Harreld, Ryuma Tanaka, Xiaoyu Li, Ji Wen, Chenran Zhang, Daniel R. Boué, Tracy M. Rauch, J. Todd Boyd, Jie Chen, Joseph C. Corbo, Thomas W. Bouldin, Scott W. Elton, Le-Wen L. Liu, Deborah Schofield, Sunhee C. Lee, John-Paul Bouffard, Maria-Magdalena Georgescu, Rimal H. Dossani, Maria A. Aguiar, Richard A. Sances, Ali G. Saad, Frederick A. Boop, Ibrahim Qaddoumi, and David W. Ellison

Department of Pathology, St Jude Children's Research Hospital, Memphis, Tennessee, USA (J.C.H.C., X.L., J.W., D.W.E.); Department of Diagnostic Imaging, St Jude Children's Research Hospital, Memphis, Tennessee, USA (J.H.H.); Department of Oncology, Division of Neuro-Oncology, St Jude Children's Research Hospital, Memphis, Tennessee, USA (R.T., I.Q.); Department of Pediatric Neurosurgery, Xinhua Hospital, School of Medicine, Shanghai Jiao Tong University, Shanghai, China (C.Z.); Department of Pathology and Laboratory Medicine, Nationwide Children's Hospital, Columbus, Ohio, USA (D.R.B.); Pathology Group of Louisiana, Baton Rouge, Louisiana, USA (T.M.R.); Clinical and Anatomic Pathology Laboratory, Dayton Children's, Dayton, Ohio, USA (J.T.B.); Department of Pathology & Immunology, Washington University School of Medicine, St. Louis, Missouri, USA (J.C., J.C.C.); Department of Pathology and Laboratory Medicine, University of North Carolina, Chapel Hill, North Carolina, USA (T.W.B.); Department of Neurosurgery, University of North Carolina, Chapel Hill, North Carolina, USA (S.W.E.); Wesley Pathology, Wichita, Kansas, USA (L-W.L.L.); Department of Pathology, Children's Hospital of The King's Daughters, Norfolk, Virginia, USA (D.S., M.A.A.); Department of Surgical Pathology, Montefiore Medical Center/Moses Campus, Bronx, New York, USA (S.C.C.); Atlantic Health System, Summit, New Jersey, USA (J-P.B.); Department of Pathology, Louisiana State University Health Science Center, Shreveport, Louisiana, USA (M-M.G.); Department of Neurosurgery, Louisiana State University Health Science Center, Shreveport, Louisiana, USA (R.H.D.); Department of Pathology, East Tennessee Children's Hospital, Knoxville, Tennessee, USA (R.A.S.); Department of Pathology, Methodist University Hospital, Memphis, Tennessee, USA (A.G.S.); Department of Surgery, Division of Pediatric Neurosurgery, St Jude Children's Research Hospital, Memphis, Tennessee, USA (C.Z., F.A.B.)

Corresponding Author: David W. Ellison, MD, PhD, Pathology, MS 250, Room C5001, St. Jude Children's Research Hospital, 262 Danny Thomas Place, Memphis, TN 38105-3678, USA (david.ellison@stjude.org).

Abstract

Background. Dysembryoplastic neuroepithelial tumors (DNETs) are uncommon neural tumors presenting most often in children and young adults and associated with intractable seizures. Rare midline neoplasms with similar histological features to those found in DNETs have been described near the septum pellucidum and termed "DNET-like neoplasms of the septum pellucidum." Due to their rarity, these tumors have been described in just a few reports and their genetic alterations sought only in small series.

Methods. We collected 20 of these tumors for a comprehensive study of their clinical, radiological, and pathological features. RNA sequencing or targeted DNA sequencing was undertaken on 18 tumors, and genome-wide DNA methylation profiling was possible with 11 tumors. Published cases (n = 22) were also reviewed for comparative purposes.

Results. The commonest presenting symptoms and signs were related to raised intracranial pressure; 40% of cases required cerebrospinal fluid diversion. Epilepsy was seen in approximately one third of cases. All patients had an indolent disease course, despite metastasis within the neuraxis in a few cases. Radiologically, the septum verum/septal nuclei were involved in all cases and are the proposed site of origin for septal DNET (sDNET). Septal DNET showed a high frequency (~80%) of mutations of platelet derived growth factor receptor A (*PDGFRA*), and alterations in fibroblast growth factor receptor 1 (*FGFR1*) and neurofibromatosis

type 1 (*NF1*) were also identified. In a genomic DNA methylation analysis alongside other neural tumors, sDNETs formed a separate molecular group.
Conclusions. Genetic alterations that are different from those of cerebral DNETs and a distinct methylome profile support the proposal that sDNET is a distinct disease entity.

Key Points

1. Septal DNET is a distinct neoplastic entity.
2. The septal nuclei are the proposed site of origin for sDNET.
3. Septal DNET shows a high frequency of *PDGFRA* mutations.

Importance of the Study

"DNET-like neoplasms of the septum pellucidum" were considered to be a variant of DNET. Our study demonstrates for the first time that the septal nuclei are the likely site of origin for sDNET. Septal DNET shows a high frequency of *PDGFRA* mutations, although alterations in *FGFR1* and *NF1* are also identified, which may have therapeutic implications. Analysis of genomic DNA methylation profiles supports sDNET as a distinct disease entity. All patients of sDNET had an indolent disease course, despite metastasis within the neuraxis in some cases.

Dysembryoplastic neuroepithelial tumors (DNETs) are neural tumors presenting most often in children and young adults with intractable seizures.[1] Rare neural tumors with similar histologic features have been described in the region of the septal nuclei and termed "DNET-like neoplasms of the septum pellucidum."[2–9] These publications have described small series of tumors or individual cases, including associated genetic alterations, but a detailed study of the disease remains to be reported.

We collected 20 DNET-like neoplasms of the septum pellucidum for a comprehensive study of their clinical, imaging, and pathological features. Gene sequencing and genome-wide DNA methylation profiling were possible with 18 and 11 tumors, respectively. Our data indicate that septal-region DNET (sDNET) is a distinct neoplasm with a high frequency (~80%) of mutations in the extracellular immunoglobulin (Ig)-like domain 4 of platelet derived growth factor receptor A (*PDGFRA*) and a putative origin in the septum verum/septal nuclei. All patients had an indolent disease course, despite metastasis within the neuraxis in some cases.

Materials and Methods

Patient Cohort

We identified 20 cases of sDNET through a search of St Jude Children's Research Hospital (SJCRH) databases. Patient demographics, clinical course, and surgical details were obtained through electronic medical records. The research was approved by the St Jude institutional review board (XPD17-050/XPD18-075).

Histopathologic Review

Standard hematoxylin and eosin histopathologic preparations from each case were supplemented by immunohistochemistry on 5 μm formalin-fixed paraffin-embedded (FFPE) tissue sections. The following antibodies were used: Ki67 (Dako, M7240, 1:100), glial fibrillary acidic protein (GFAP) (Ventana, 6F2, 1:400), oligodendrocyte transcription factor (Olig2) (Cell Marque, 387M-15, 1:50), synaptophysin (Leica Microsystems, NCL-L-SYNAO-299, 1:400), and neurofilament protein (Ventana, 2F11, prediluted).

Imaging Review

MR images were available for review in 17/20 cases. A further 2 had only postoperative imaging, precluding evaluation of the presenting tumor. The tumors were evaluated for location (involvement of the septal nuclei, septum pellucidum, fornices, subcallosal area, and anterior commissure), T1/T2/T2 fluid attenuated inversion recovery (FLAIR) signals, enhancement, and apparent diffusion coefficient (ADC) relative to the thalamus, calculated as $ADC_{tumor}/ADC_{thalamus}$.[10] The boundaries of the septum verum, which contains the Ch1 and Ch2 septal nuclei, were defined according to criteria reported by Butler et al.[11] On MRI, these nuclei are delimited anteriorly by a line connecting the anterior margins of the globi pallidi, laterally by a vertical line extending inferiorly to the base of the brain from the inferomedial boundary of the lateral ventricle, superiorly by the membranous septum pellucidum, and posteriorly by the fornices.

RNA Extraction, Sequencing, and Analysis

The PureLink FFPE Total RNA Isolation Kit (Thermo Fisher Scientific) was used for total RNA extraction from archived FFPE tissue sections ($n = 10$). Purified RNA was quantitated on a Qubit 1.27 fluorometer (Thermo Fisher Scientific) using the Qubit RNA BR Assay Kit (Thermo Fisher Scientific). Total RNA sequencing used the Illumina Total Stranded RNA protocol with at least 400 ng of total RNA. The quality of the

starting materials was checked with the RNA 6000 Nano Assay on a 2100 Bioanalyzer (Agilent) or the RNA Pico Sensitivity Assay on a LabChip GX Touch (PerkinElmer). Libraries were prepared using the TruSeq Stranded Total RNA Sample Prep Kit (Illumina), followed by library quantification through quantitative PCR using Quant-iT PicoGreen dsDNA Assay Kits (Thermo Fisher Scientific) or KAPA Library Quantification Kits for Illumina platforms, and through low pass sequencing on a MiSeq Nano v2 (Illumina). All sequencing data were generated after 100 cycles of paired end runs on an Illumina HiSeq 2500 or HiSeq 4000. The RNA-seq data were aligned to human reference genome (build hg19), as previously described.[12] The single nucleotide variants were discovered using Bambino,[13] annotated and ranked by putative pathogenicity using a workflow named "medal ceremony,"[14] and then manually reviewed.

Targeted DNA Sequencing

For samples with insufficient material for RNA-seq, genetic alterations were interrogated by targeted PCR followed by Sanger sequencing (n = 8). Genomic DNA or cDNA was used as the template. PCR products were purified with Monarch PCR & DNA Cleanup Kit (New England Biolabs). Primer sequences for amplification and sequencing are listed in Supplementary Table 1.

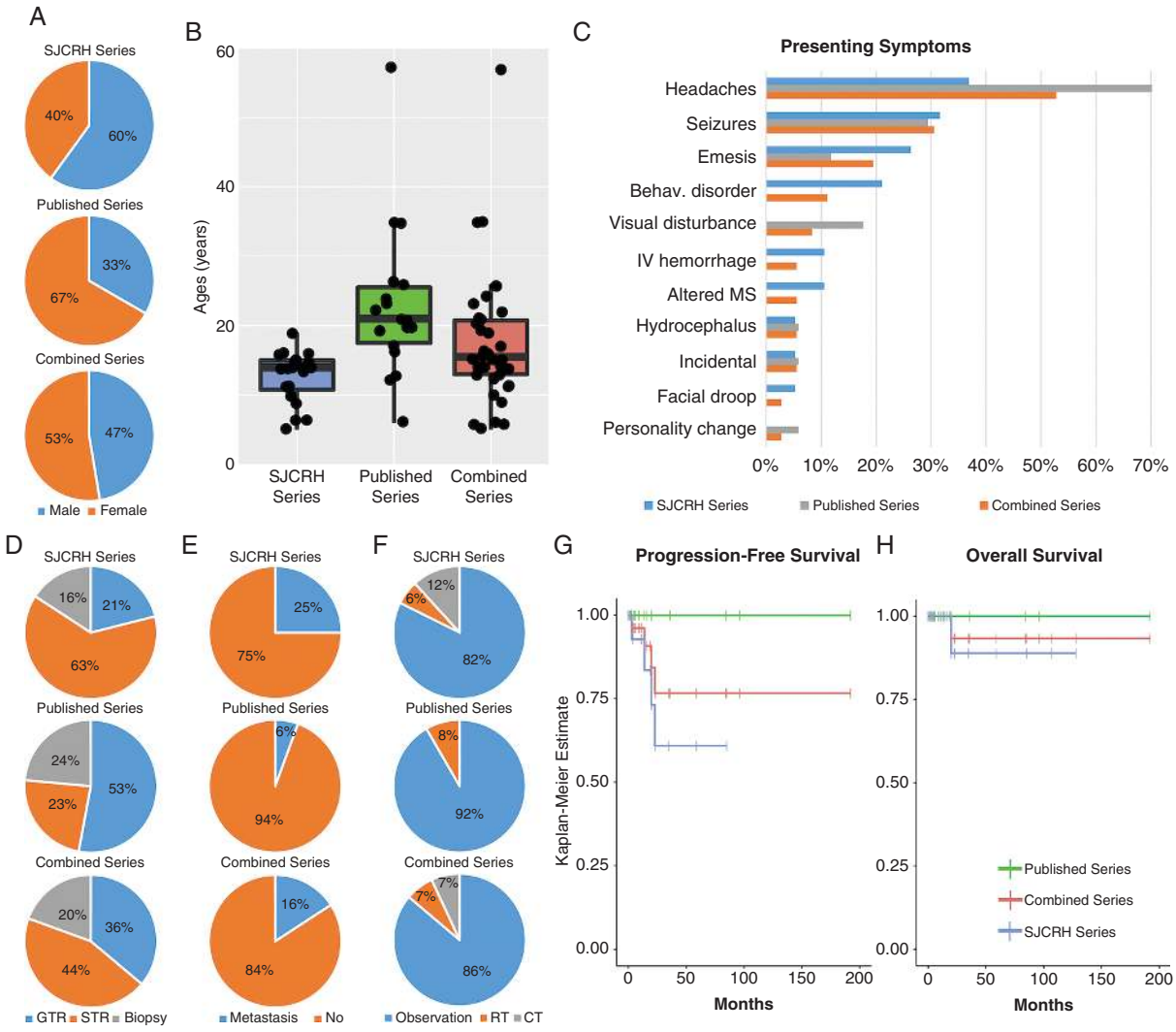

Fig. 1 Clinical Features of sDNET. (A) Although the SJCRH series shows slight male predilection, there is no gender predilection in the combined series. (B) Box and scatter plots of age at diagnosis. (C) Frequencies of presenting symptoms; MS = mental status, IV = intraventricular. (D) Due to its location, gross total resection (GTR) of sDNET was possible in only a portion of cases. STR = subtotal resection. (E) Cases showed metastasis within the neuraxis at presentation or during follow-up. (F) Most cases of sDNET were managed by observation alone after surgery. (G) Progression-free survival of patients with sDNET; median time to progression was 19 months for the SJCRH series. (H) Overall survival of patients with sDNET.

DNA Extraction, Methylation Profiling, and Analysis

Genomic DNA extracted from available FFPE tissue samples using a QIAamp DNA FFPE Tissue Kit (Qiagen) was used to generate DNA methylation data on Illumina Infinium MethylationEPIC BeadChip arrays according to the manufacturer's instructions. At least 250 ng of DNA was used for most FFPE tissues. DNA samples were checked for quality using the Infinium HD FFPE QC Assay Protocol, followed by bisulfite conversion using the EZ-96 DNA Methylation Kit (Zymo Research). The purified converted

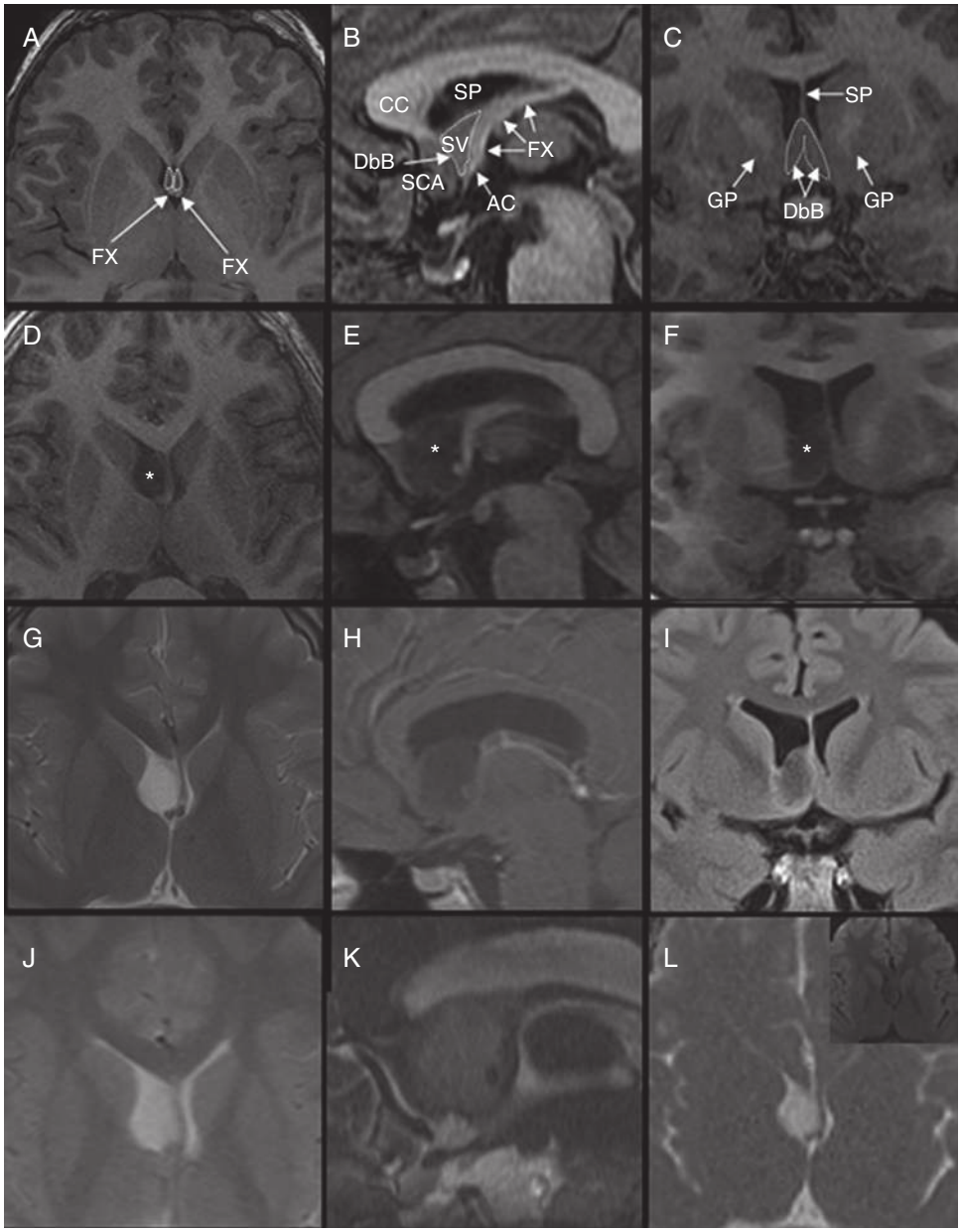

Fig. 2 Anatomy of sDNET. (A) Axial, (B) sagittal, and (C) coronal T1-weighted images (T1WI) show the normal anatomy of the septum verum (SV) and surrounding structures. The diagonal band of Broca (DbB, containing Ch2 nuclei) is visible at the anterior, medial, and inferior aspect of the SV. The septum pellucidum (SP) is a thin membrane above the SV. CC = corpus callosum, FX = fornix, AC = anterior commissure, SCA = subcallosal area, GP = globi pallidi. Typical sDNET (*) located in the SV, in this case on the right, is shown on (D) axial, (E) sagittal, and (F) coronal T1WI. Typically, sDNET appears hyperintense on T2-weighted images (G) and non-enhancing on T1WI with contrast (T1WI+C) (H), and partially suppressed on T2-weighted FLAIR images (I). (J) Axial gradient recalled echo images show no susceptibility suggestive of hemorrhage. (K) Sagittal images from FIESTA (Fast Imaging Employing Steady-state Acquisition) show almost fluid-like signal. (L) On ADC map, the tumor is hyperintense, consistent with absence of restricted water diffusion seen as low signal on diffusion-weighted image (inset).

DNA was then restored, following the Infinium HD FFPE Restore Protocol, to a state amplifiable by the Infinium HD FFPE methylation whole genome amplification protocol. After whole genome amplification, endpoint fragmentation, and cleanup, the DNA samples were hybridized onto the BeadChips overnight in the Illumina Hybridization Oven, followed by washing, single-base extension, and staining. Finally, the BeadChips were scanned by the iScan System in the setting of Methylation NXT.

DNA methylation profiles generated with the Illumina Infinium HumanMethylation450 (450K) array from low-grade neuroepithelial tumors, including angiocentric glioma, diffuse astrocytoma, cortical DNET, pediatric oligodendroglioma/oligoastrocytoma, were used in a comparative analysis of available sDNETs. Common probes from both 450K and EPIC arrays were identified, corrected for background values, and then normalized with the SWAN method using the minfi package v1.24.0.[15] The 1000 most variable methylation probes were selected by standard deviation. A consensus clustering was performed using the ConsensusClusterPlus package v1.24.0.[16] The following nondefault parameters were used: maxK = 10, rep = 1000, distance = "euclidean," innerLinkage = "ward.D2," pItem = 0.5 and pFeature = 0.5. The first 50 principal components were used for t-SNE (t-Distributed Stochastic Neighbor Embedding) analysis using the Rtsne package v0.13. The following nondefault parameters were used: theta = 0, pca = F, max_iter = 5000, and perplexity = 8. Copy-number variation analysis was performed with the conumee package v1.14.0.[17]

Results

Clinical Features

Following a search for potential cases, 20 sDNETs were included in the SJCRH series on the basis of their common anatomic location and histologic features. This series was compared with 18 reported cases (the published series), all tumors with a similar anatomic location and histologic features to the SJCRH series. The clinical features of the SJCRH, published, and combined (n = 38) series are summarized in Fig. 1 and Supplementary Table 2.

Most patients presented with symptoms related to raised intracranial pressure. In the SJCRH series, 65% (13/20) of cases had some degree of hydrocephalus and 40% (8/20) required ventriculoperitoneal shunt placement. Epilepsy occurred in approximately one third of patients. Behavioral disorders—including attention deficit hyperactivity disorder, oppositional defiant disorder, significant academic decline, and emotional outbursts—were documented in 4 patients. Two patients presented with intraventricular hemorrhage, and the diagnosis of sDNET was made 4 or 5 years after the surgery to evacuate hematoma.

Due to the anatomic relationships of the tumors, gross total resection was possible in only a minority of cases. After tumor resection or biopsy, patients were initially managed by observation alone, except for 1 patient in the SJCRH series, who received craniospinal irradiation for disseminated disease, and 1 patient from the published series, who received focal radiation.[3] In the SJCRH series, 4 patients developed pituitary hormone deficiency, including hypothyroidism, adrenal insufficiency, hypogonadism, or diabetes insipidus, as a complication of surgery. Chemotherapy—vincristine and carboplatin—was given to 2 patients in the SJCRH series at disease progression after 14 or 23 months. Both patients maintained stable disease for a long time thereafter. All other patients maintained stable disease without receiving radiation or chemotherapy.

Progression-free and overall survival curves were plotted for the SJCRH published and combined series (Fig. 1G, H). Median time to progression was 19 months for the SJCRH series. While a recurrence occurred in several patients, only 2 of the combined series of patients died, both of causes unrelated to the tumor.

Imaging Findings of sDNET

The characteristic imaging findings of sDNET are shown in Fig. 2. Images of sDNET in the SJCRH series are shown in Supplementary Fig. 1. The septum verum/septal nuclei were involved by the neoplastic process in all 15 SJCRH patients

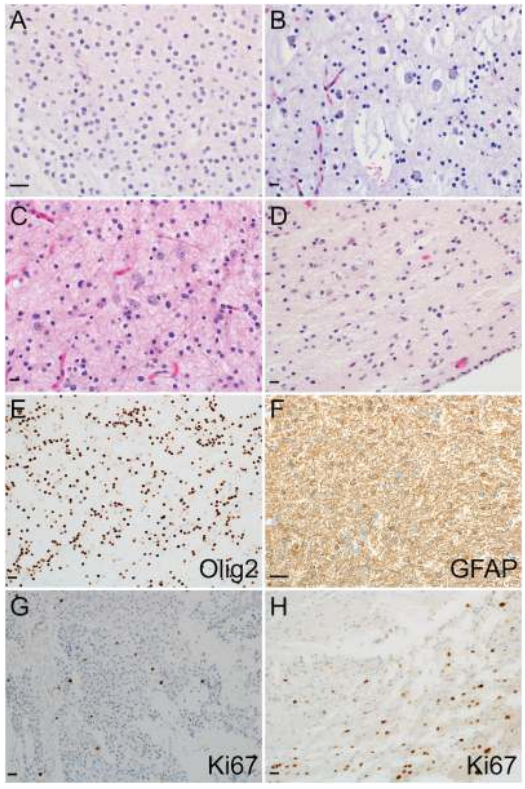

Fig. 3 Characteristic histopathologic and immunophenotype of sDNET. (A) The presence of numerous OLCs is a feature of sDNET. (B) Neurons that appear to "float" in mucin pools are an uncommon finding. (C) Septal DNET has a tendency for an infiltrative growth pattern, revealed by the presence of numerous entrapped axons and neurons. (D) Infiltration beneath the ependyma is also another characteristic finding. (E) The tumor cells in sDNET are positive for Olig2 and GFAP (F). (G) Ki67 immunolabeling is generally low but can reach a moderate level in focal areas in a few cases (H). Scale bar = 50 µm.

with available imaging and in 18 published cases based on imaging ($n = 9$)[2,3,6–8,18] or a detailed description of tumor location ($n = 9$).[2] The septum pellucidum was involved in less than half (7/15) of the cases in the SJCRH series.

Similar to cortical DNETs, all except one hemorrhagic tumor showed fluid-like low signal on T1-weighted images (T1WI) and high signal on T2-weighted images. T2 FLAIR signals were low (fluid signal nearly completely suppressed) or moderate (incomplete suppression). ADC relative to the thalamus was >3 (mean 3.27 ± 0.19) in all tumors with quantitative ADC maps, consistent with relatively free diffusion of fluid. Only 2 of 13 tumors evaluated with gadolinium contrast-enhanced T1WI (T1WI+C) showed small nodular enhancement; otherwise, none enhanced. Among the 13 subjects with documented hydrocephalus, imaging studies were available for review in 12 cases; 7 had obstruction at the foramen of Monro, and another 5 had compensated ventriculomegaly, suggesting long-standing, at least partial, obstruction. Only 4 of 15 had normal ventricular size. Calcification, a common feature of cortical DNETs, was not seen. Prominent peritumoral edema was not a feature of the disease. In the SJCRH series, intraventricular dissemination was seen in 3 patients at presentation; one later developed extensive leptomeningeal disease. One additional case had documented leptomeningeal metastasis, but imaging was not available for review.

Histopathologic Findings and Immunophenotype

The morphologic features and immunophenotype of tumors in the SJCRH series are illustrated in Fig. 3. Macroscopically, sDNET appears as a gelatinous subependymal mass (Supplementary Video 1). On histologic examination, tumor cells have an oligodendrocyte-like morphology with round to oval nuclei, often accompanied by perinuclear cytoplasmic clearing. Oligodendrocyte-like cells (OLCs) infiltrate adjacent brain tissue, where a mucin-rich matrix and microcysts are often observed. The nodular architecture and "specific glioneuronal element" characteristic of cortical DNETs are not found. Eosinophilic granular bodies and Rosenthal fibers are rare findings. OLCs in sDNETs express Olig2 and, unlike cortical DNETs, commonly show diffuse immunoreactivity for GFAP. OLCs do not express neuronal proteins. Mitotic Figures are rare,

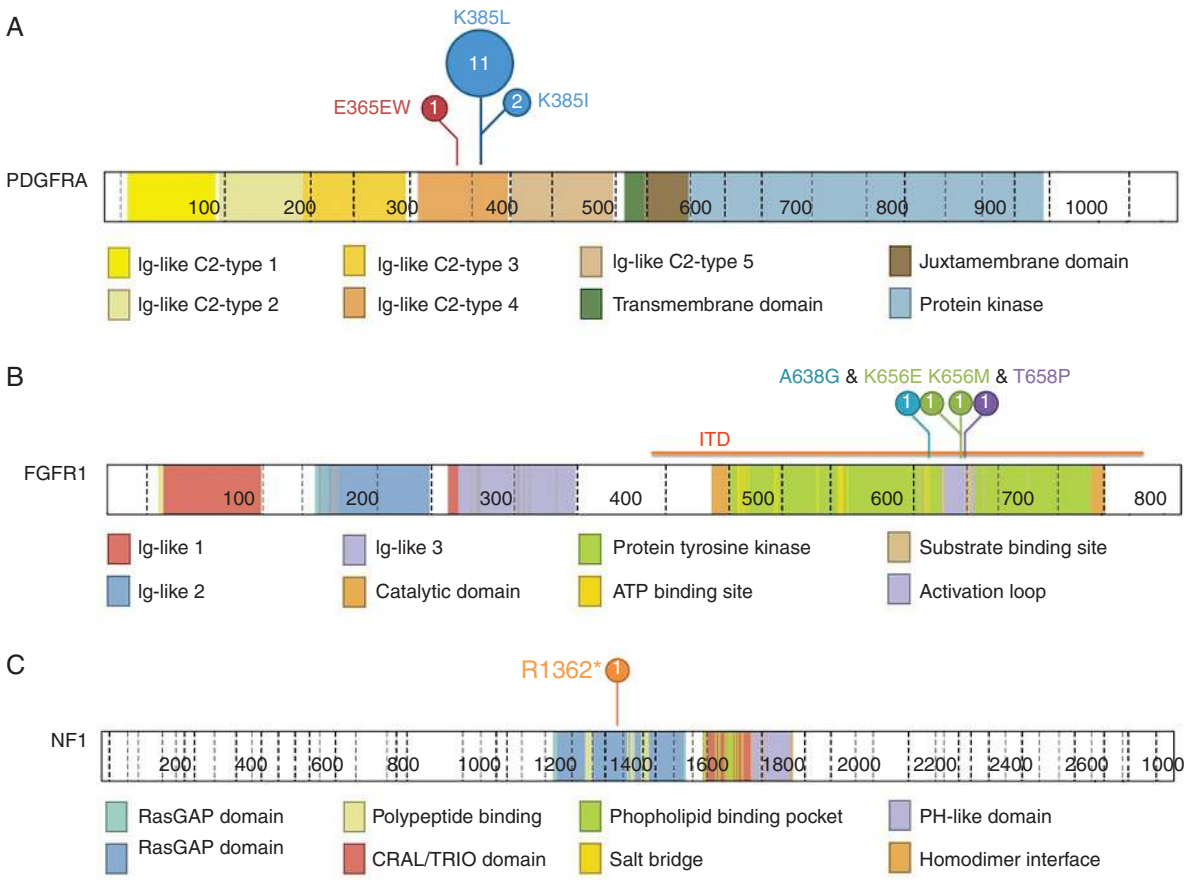

Fig. 4 Molecular alterations in sDNET. Nearly 80% (14/18) of tumors with available tissue for sequencing harbor alterations in PDGFRA Ig-like domain 4, especially in the K385 residue (13/14, 92.9%). (B) FGFR1 alterations, including hotspot double mutations (K656E and A638G, and K656M and T658P) in the tyrosine kinase domain (TKD) and internal tandem duplication (ITD) of the TKD are found in 3 other tumors. (C) An NF1 mutation in the Ras-GTPase activating (GAP) domain is identified in 1 tumor; number of cases in circles. Diagram and domain information were obtained from Pediatric Cancer Data Portal (PeCan) of St Jude Children's Research Hospital (https://pecan.stjude.cloud/home).

and Ki67 immunolabeling is generally low. Cortical dysplasia in the adjacent brain areas was not a feature of the tumors in the SJCRH series.

Septal DNET Harbors Recurrent PDGFRA Mutations

Single pathologic mutations were identified in all 18 tumors with sufficient material for sequencing (Fig. 4). Nonsynonymous *PDGFRA* mutations within the extracellular Ig-like C2-type domain 4 were present in 14/18 (77.8%) sDNETs. Hotspot fibroblast growth factor receptor 1 (*FGFR1*) double mutations in the tyrosine kinase domain (TKD) were seen in 2/18 (11.1%) and an internal tandem duplication (ITD) of the *FGFR1* TKD in 1. An NF1:p.R1362* nonsense mutation in the Ras-GTPase activating domain was found in one sDNET from a patient who showed no clinical signs of NF1. Of 14 tumors with a *PDGFRA* mutation, 13 (92.9%) had alterations in the K385 residue. Eleven (84.6%) had a PDGFRA:p.K385L mutation, and 2 had a PDGFRA:p.K385I mutation. Another tumor had a PDGFRA:p.E365EW insertion within the same domain. Structural variants were not identified. Alterations in isocitrate dehydrogenase 1 and 2 or *BRAF* were not detected.

DNA Methylation Profiling of sDNET

An unsupervised cluster analysis and t-SNE plot based on genomic DNA methylation profiling support the proposal that sDNET is a tumor with a distinct histogenesis (Fig. 5); 9 of 11 tumors form a distinct cluster in both analyses compared with a range of similar low-grade neural tumors. The remaining 2 tumors cluster closely with low-grade neural tumors that have *BRAF* or *FGFR1* alterations. Although a *PDGFRA* mutation at the K385 residue is present in 2 cortical DNETs, these tumors do not cluster with the sDNETs. Similar to other pediatric low-grade neural tumors, sDNETs show minimal copy number variations (data not shown).

Discussion

DNETs are rare low-grade neural tumors located in the cerebral cortex and characterized histologically by OLCs.[19] Exceptionally rare tumors with similar histologic features have been described in the region of the septal nuclei and termed DNET-like neoplasms of the septum pellucidum,[2–9] although our radiological findings suggest that the septal nuclei are a more likely site of origin for sDNET. Our findings also show that, while some pathologic and imaging

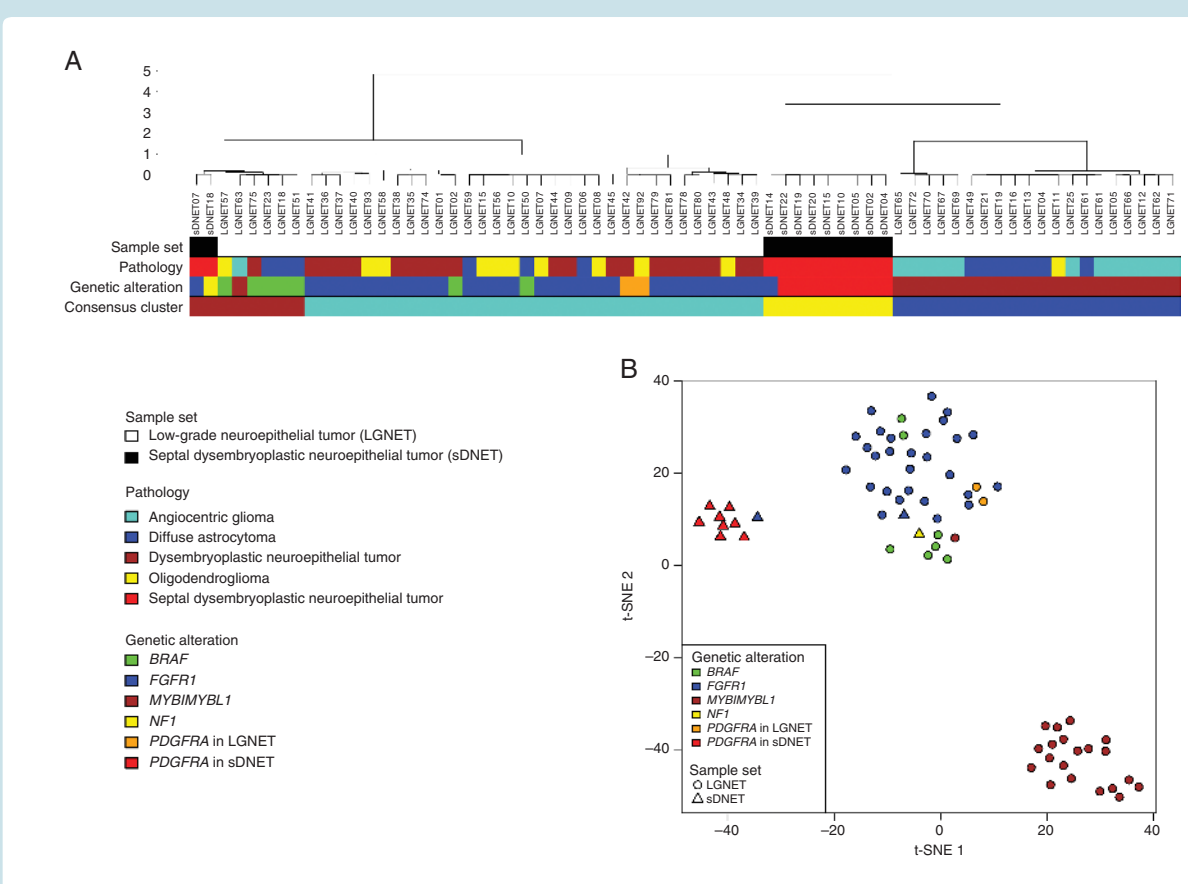

Fig. 5 Septal DNET is a molecularly distinct entity. Both unsupervised cluster analysis (A) and a t-SNE plot (B) of methylation profiles of sDNET and pediatric low-grade neuroepithelial tumors (LGNETs) highlighted sDNET as a molecularly distinct disease entity; AG = angiocentric glioma, DA = diffuse astrocytoma, O = oligodendroglioma.

characteristics of sDNET and cortical DNET overlap, their clinical features, which are largely dictated by anatomic site, demonstrate differences. Cortical DNETs are characteristically associated with epilepsy, which is sometimes intractable. However, epilepsy occurred in only one third of patients with sDNET; raised intracranial pressure was the commonest mode of presentation. Outcomes for cortical DNETs and sDNETs appear similar; both are associated with relapse in a minority of patients but have good overall survivals.

Cortical DNETs and sDNETs also show morphologic differences. Data from our series and from published reports indicate that the microscopic nodular architecture and "specific glioneuronal element" of cortical DNETs are not seen in sDNET. In addition, the glial nodules of complex DNETs were not identified in our series, and "floating neurons" were rare. Tumor cells in cortical DNETs are typically immunonegative for GFAP, but expression of GFAP highlighting the cytoplasmic processes of tumor cells was a common finding in our sDNET series.

Limited nucleic acid derivatives from FFPE tissue determined our approach to sequencing. For half our sDNET series, it was possible to extract RNA of sufficient quality for total RNA sequencing, enabling a transcriptome-wide perspective of genetic alterations in these tumors. Subsequent analysis revealed a solitary pathologic mutation in all 10 tumors sequenced in this way and helped to orient our approach to targeted sequencing. Using both methods, we identified a high frequency (~80%) of mutated *PDGFRA* in sDNET, and mutations in the K385 residue dominated these results. *PDGFRA* alterations are rare in pediatric low-grade neural tumors[12]; therefore, the enrichment of *PDGFRA* mutations at a specific amino acid residue is a notable finding. *PDGFRA* mutations in sDNETs were found exclusively in the extracellular Ig-like C2-type 4 domain, which mediates the receptor-receptor interaction required for dimerization and activation upon binding of PDGFs,[20] suggesting a gain-of-function role with these mutations. *FGFR1* alterations, including hotspot mutations and a TKD ITD, have been reported in cortical DNETs and pediatric-type oligodendrogliomas. These also occur in sDNET, but at much lower frequencies, further setting sDNET apart from the cortical DNET.

The distinctive mutational profile of sDNET is matched by its DNA methylation profile. The great majority of sDNETs in our analysis formed a distinct group in unsupervised cluster analysis and in a t-SNE plot compared with other low-grade neural tumors, notably cortical DNETs and pediatric oligodendrogliomas with similar *PDGFRA* and *FGFR1* alterations. Altogether, our findings support septal DNET as a disease with distinctive clinicopathological and molecular features.

Supplementary Material

Supplementary data are available at *Neuro-Oncology* online.

Keywords

DNET | *FGFR1* | *NF1* | *PDGFRA* | septum verum

Funding

This work was supported by the American Lebanese Syrian Associated Charities (ALSAC).

Acknowledgments

The authors would like to thank Emily Walker, Rain Sun, and Scott Olsen of the St Jude Hartwell Center for their technical support with genomic DNA methylation profiling and RNA sequencing; Matthew Lear of the St Jude Biorepository for his assistance in providing study material; Raven Holcomb and Alice Slusher in the St Jude Pathology Department for their assistance with specimen processing; and Dianne Scott and Stacey Davis in the St Jude Pathology Department for administrative assistance. This work has been supported by St Jude and the American Lebanese Syrian Associated Charities and in part by an NIH grant to DWE - CA096832.

Conflict of interest statement. The authors declare no conflict of interest.

Authorship statement: Experimental design: JCHC, DWE Implementation: JCHC, JHH, XL, CZ, DRB, TMR, JTB, JC, JCC, TWB, SWE, LWLL, DS, SCL, JPB, MMG, RHD, MAA, RAS, AGS, FAB Imaging review: JHH Pathology review: JCHC, DWE Review of clinical information: RT, JCHC, IQ Analysis and interpretation of the data: JCHC, JHH, RT, JW, DWE Writing of the manuscript: JCHC, JHH, RT, XL, JW, DWE All authors have read and approved the final version.

References

1. Nolan MA, Sakuta R, Chuang N, et al. Dysembryoplastic neuroepithelial tumors in childhood: long-term outcome and prognostic features. *Neurology.* 2004;62(12):2270–2276.
2. Baisden BL, Brat DJ, Melhem ER, Rosenblum MK, King AP, Burger PC. Dysembryoplastic neuroepithelial tumor-like neoplasm of the septum pellucidum: a lesion often misdiagnosed as glioma: report of 10 cases. *Am J Surg Pathol.* 2001;25(4):494–499.
3. Cervera-Pierot P, Varlet P, Chodkiewicz JP, Daumas-Duport C. Dysembryoplastic neuroepithelial tumors located in the caudate nucleus area: report of four cases. *Neurosurgery.* 1997;40(5):1065–1069; discussion 1069–1070.
4. Daghistani R, Miller E, Kulkarni AV, Widjaja E. Atypical characteristics and behavior of dysembryoplastic neuroepithelial tumors. *Neuroradiology.* 2013;55(2):217–224.
5. Gessi M, Hattingen E, Dörner E, et al. Dysembryoplastic neuroepithelial tumor of the septum pellucidum and the supratentorial midline: histopathologic, neuroradiologic, and molecular features of 7 cases. *Am J Surg Pathol.* 2016;40(6):806–811.

6. Harter DH, Omeis I, Forman S, Braun A. Endoscopic resection of an intraventricular dysembryoplastic neuroepithelial tumor of the septum pellucidum. *Pediatr Neurosurg.* 2006;42(2):105–107.
7. Ongürü O, Deveci S, Sirin S, Timurkaynak E, Günhan O. Dysembryoplastic neuroepithelial tumor in the left lateral ventricle. *Minim Invasive Neurosurg.* 2003;46(5):306–309.
8. Wang F, Qiao G, Li X, Gui Q. A dysembryoplastic neuroepithelial tumor in the area of the caudate nucleus in a 57-year-old woman: case report. *Neurosurgery.* 2007;61(2):E420; discussion E420.
9. Xiong J, Liu Y, Chu SG, et al. Dysembryoplastic neuroepithelial tumor-like neoplasm of the septum pellucidum: review of 2 cases with chromosome 1p/19q and IDH1 analysis. *Clin Neuropathol.* 2012;31(1):31–38.
10. Koral K, Alford R, Choudhury N, et al. Applicability of apparent diffusion coefficient ratios in preoperative diagnosis of common pediatric cerebellar tumors across two institutions. *Neuroradiology.* 2014;56(9):781–788.
11. Butler T, Harvey P, Deshpande A, et al. Basal forebrain septal nuclei are enlarged in healthy subjects prior to the development of Alzheimer's disease. *Neurobiol Aging.* 2018;65:201–205.
12. Qaddoumi I, Orisme W, Wen J, et al. Genetic alterations in uncommon low-grade neuroepithelial tumors: BRAF, FGFR1, and MYB mutations occur at high frequency and align with morphology. *Acta Neuropathol.* 2016;131(6):833–845.
13. Edmonson MN, Zhang J, Yan C, Finney RP, Meerzaman DM, Buetow KH. Bambino: a variant detector and alignment viewer for next-generation sequencing data in the SAM/BAM format. *Bioinformatics.* 2011;27(6):865–866.
14. Mistry M, Zhukova N, Merico D, et al. BRAF mutation and CDKN2A deletion define a clinically distinct subgroup of childhood secondary high-grade glioma. *J Clin Oncol.* 2015;33(9):1015–1022.
15. Aryee MJ, Jaffe AE, Corrada-Bravo H, et al. Minfi: a flexible and comprehensive Bioconductor package for the analysis of Infinium DNA methylation microarrays. *Bioinformatics.* 2014;30(10):1363–1369.
16. Wilkerson MD, Hayes DN. ConsensusClusterPlus: a class discovery tool with confidence assessments and item tracking. *Bioinformatics.* 2010;26(12):1572–1573.
17. Hovestadt V, Zapatka M. conumee: enhanced copy-number variation analysis using Illumina DNA methylation arrays, http://bioconductor.org/packages/conumee/. Accessed August 27, 2018.
18. Yuan J, Sharma N, Choudhri H, Figueroa R, Sharma S. Intraventricular dysembryoplastic neuroepithelial tumor in a pediatric patient: is it the most common extracortical location for DNT? *Childs Nerv Syst.* 2011;27(3):485–490.
19. Campos AR, Clusmann H, von Lehe M, et al. Simple and complex dysembryoplastic neuroepithelial tumors (DNT) variants: clinical profile, MRI, and histopathology. *Neuroradiology.* 2009;51(7):433–443.
20. Omura T, Heldin CH, Ostman A. Immunoglobulin-like domain 4-mediated receptor-receptor interactions contribute to platelet-derived growth factor-induced receptor dimerization. *J Biol Chem.* 1997;272(19):12676–12682.